Estimating and improving the signal-to-noise ratio of time series by symbolic dynamics

Peter beim Graben*

Institute of Linguistics, Universität Potsdam, P.O. Box 601553, D-14415 Potsdam, Germany

We investigate the effect of symbolic encoding applied to times series consisting of some deterministic signal and additive noise, as well as time series given by a deterministic signal with randomly distributed initial conditions as a model of event-related brain potentials. We introduce an estimator of the signal-to-noise ratio (SNR) of the system by means of time averages of running complexity measures such as Shannon and Rényi entropies, and prove its asymptotical equivalence with the linear SNR in the case of Shannon entropies of symbol distributions. A SNR improvement factor is defined, exhibiting a maximum for intermediate values of noise amplitude in analogy to stochastic resonance phenomena. We demonstrate that the maximum of the SNR improvement factor can be shifted toward smaller noise amplitudes by using higher order Rényi entropies instead of the Shannon entropy. For a further improvement of the SNR, a half wave encoding of noisy time series is introduced. Finally, we discuss the effect of noisy phases on the linear SNR as well as on the SNR defined by symbolic dynamics. It is shown that longer symbol sequences yield an improvement of the latter.

I. INTRODUCTION

In signal analysis one often assumes that a measured time series $x(t)$ consists of a deterministic signal $s(t)$ and some additive noise $\xi_\sigma(t)$ with variance σ^2:

$$x(t) = s(t) + \xi_\sigma(t). \tag{1}$$

This assumption is also maintained in analyzing event-related brain potentials (ERP's), where $s(t)$ is regarded to be an invariant response of the brain to certain stimuli that is obscured by the brain's spontaneous activity and observational noise, both described by an additive noise term $\xi_\sigma(t)$ [1–4]. In order to regain the invariant ERP signal $s(t)$ from an ensemble of measured EEG epochs $x_i(t)$, where i denotes an ensemble index ranging across all measured trials N, $1 \leq i \leq N$, the noise is requested to be stationary as well as ergodic [5]. Then the signal can be estimated by the ensemble average

$$\bar{x}(t) = \frac{1}{N} \sum_{i=1}^{N} x_i(t).$$

A well known characteristic of the quality of a measurement is the signal-to-noise ratio (SNR), given by the ratio of the signal power over the power of noise [6],

$$Q = \sqrt{\frac{P_S}{P_N}}, \tag{2}$$

with

$$P_S = \frac{1}{T} \int_0^T s^2(t) dt \tag{3}$$

and

$$P_N = D^2(\xi_\sigma(t)) = \sigma^2, \tag{4}$$

where T denotes the duration of the time series. There have been several suggestions of how to estimate the SNR of event-related brain potentials, e.g., by computing correlation coefficients [7] or coherence measures [8], or by dividing the amplitude of averaged ERP wave forms by the standard deviation of the prestimulus interval [9,10]. Möcks *et al.* [11] suggested an ansatz that is mostly related to Eqs. (3) and (4)

$$\hat{P}_S = \frac{1}{T} \int_0^T \bar{x}^2(t) dt - \frac{1}{N} \hat{P}_N, \tag{5}$$

$$\hat{P}_N = \frac{1}{N-1} \sum_{i=1}^{N} \frac{1}{T} \int_0^T (x_i(t) - \bar{x}(t))^2, \tag{6}$$

where we denoted statistical estimates by a hat. When the noise is neither correlated with the signal nor with itself across trials, averaging yields an improvement of the SNR by $\sqrt{N}$ [3].

It is commonly accepted in the literature that none of the assumptions given above are really met in EEG data. The background EEG cannot be regarded as stationary and ergodic noise [12,11], but that it is somehow correlated with the brain's responses to certain stimuli; these responses are not invariant in time because they change in amplitude, scalp distribution, and morphology as well as in latency time (i.e., the signal onset time), e.g., caused by habituation, learning or by changes in attention [7,11–16]. Finally, the ansatz [Eq. (1)] states that there is no impact of the noise on the dynamics of the EEG. It is assumed to be purely observational noise.

In measured ERP data there is also an additional source of noise, called latency jitter. This means that the ERP signal $s(t)$ is randomly shifted in time by some random variable τ [5,9], obeying

---

*Email address: peter@ling.uni-potsdam.de; also at Inst. of Physics, Nonlinear Dynamics Group.

$$x(t) = s(t + \tau). \tag{7}$$

Improving the SNR of measured time series is also a common job of data analysis. This is traditionally achieved by using linear filters suppressing energy of certain frequency bands of the noise spectrum [6]. In the last years the phenomenon of stochastic resonance (SR) has drawn considerable attention [17–19]. A similar phenomenon, noise induced threshold crossings [20–22] occur in nonlinear threshold devices which are fed by noisy periodic or broadband signals. In the latter case one speaks of *aperiodic stochastic resonance* [23–25]. Experimentally, SR becomes manifest as a maximum of the SNR depending on the noise amplitude. Gong and co-workers therefore proposed using electronic stochastic resonance devices such as Schmitt triggers [26] for enhancing the SNR of measured data [27–29].

Recently, we developed a data analysis technique that overcomes the strong requirements of traditional ERP analysis, resting on symbolic dynamics and measures of complexity [5]. We suggested considering event-related brain potentials in terms of dynamical system theory, and presented a theoretical framework for dealing with nonstationary stochastic dynamical systems. Symbolic dynamics belongs to the mathematical theory of dynamical systems, describing states and trajectories by symbolic sequences obtained from a partition of the system's state space [30,31]. However, symbolic dynamics has also been successfully applied to analyze natural data during the last decade [32–42]. It has often been claimed in the literature that symbolic dynamics leaves ''robust'' properties of dynamical systems invariant [31,35,43] by ''ignoring information about the details of the trajectory in phase space'' [33]. When the ''details'' are contributed by noise, symbolic dynamics can be regarded as some filtering technique. The impact of noise on symbolic dynamics of nonlinear systems was studied in Refs. [5,42–45].

In this paper we demonstrate that symbolic dynamics is a powerful approach of data analysis even under the assumptions of traditional ERP research. We consider noisy data of the type of Eq. (1), where $s(t)$ might be any periodic or aperiodic ERP-like signal, in connection with a threshold device as an unique physical system (in analogy to the measurement process in quantum mechanics) in order to obtain a symbolic dynamics of the joined process. We show that no additional electronic devices are needed for enhancing the signal component of the data. The organization of the paper is as follows. In Sec. II we introduce the basic concepts of symbolic dynamics applied to time series analysis, mainly the notion of cylinder sets and measures of complexity. In Sec. III we shall discuss the symbolic dynamics of Eq. (1) leading to a formula for estimating the SNR [Eq. (2)] of the system by the time average of running cylinder entropies. We compare analytical results with results from numerical simulations. We show that Rényi entropies are able to improve the SNR of the system considerably in contrast to the Shannon entropy. Then, we introduce an alternative method of symbolic encoding, detecting half waves of the noisy signal Eq. (1). Using this encoding technique, we obtain a further improvement of the SNR. In Sec. IV we discuss the symbolic dynamics of the latency jitter [Eq. (7)]. In Sec. IV A we compute the damping of signals in the presence of latency noise analytically. Section IV B is devoted to theoretical as well as numerical considerations of the symbolic dynamics. Here we demonstrate that higher word order statistics and their related measures of complexity are appropriate for improving the SNR of systems with randomly distributed initial conditions.

II. SYMBOLIC DYNAMICS

Let us consider an ensemble of real valued time series $x_i(t)$ obtained by a measurement of some natural system, where i ($1 \leq i \leq N$) is the ensemble index and t is the (discrete) time index ranging from 1 to L. N is the cardinality of the ensemble. Subsequently, we shall refer to $x_i(t)$ as *trials*, *epochs*, or *realizations* of a stochastic dynamical system. In order to gain a symbolic dynamics of the ensemble, one has to partitionate the state space of the underlying system into a finite number of pairwise disjunct subsets; these subsets are assigned to letters of a finite set, called an *alphabet*. Though for experimental data the state space is generally unknown and has to be reconstructed from measured time series by delay embedding techniques [46]. In Ref. [5] we showed that every partition of the set of measurement values yields a partition of the state space automatically. The simplest way of constructing a symbolic dynamics is to use a certain binning of the range of $x_i(t)$ into two or more nonoverlapping intervals. This procedure is called *static encoding* of the time series [47]. A binary static encoding partitionates the range of measurement values into two subsets by using a threshold θ [32,35,43]. The encoding rule

$$s_{i;t} = \begin{cases} 0: & x_i(t) < \theta_i \\ 1: & x_i(t) \geq \theta_i \end{cases} \tag{8}$$

maps each value $x_i(t)$ of the ith time series at time t to ''0'' if $x_i(t)$ is below the threshold θ_i, and to ''1'' otherwise. The threshold should depend on the ensemble index i because some statistic properties of $x_i(t)$ might differ from trial to trial. For experimental data, θ_i can be chosen as a time average of the realization $x_i(t)$ [43] or, as we did, as the median of $x_i(t)$ [5].

By using the encoding rule [Eq. (8)] we obtain a matrix $(s_{i;t})_{i \leq N; t \leq L}$ of symbols ''0'' and ''1.'' The rows of this matrix are images of the epochs $x_i(t)$ under the symbolic encoding. Thus the matrix $(s_{i;t})_{i \leq N; t \leq L}$ can be considered as a set of rows

$$E = \{ s_i | s_i \in \{0,1\}^L, 1 \leq i \leq N \}, \tag{9}$$

where $\{0,1\}^L$ denotes the Lth Cartesian power of the alphabet $\{0,1\}$. Now, we introduce the most important concept of our approach. A subset C of the ensemble E is called an n-cylinder at time t, if there are n letters $a_{i_1}, \ldots, a_{i_n} \in \{0,1\}$, and a time point t such that all sequences in the subset C match in the subsequence $a_{i_1}, \ldots, a_{i_n} \in \{0,1\}$ beginning at time t. Or, formally,

$$C = [a_{k_1}, \dots, a_{k_n}]_t = \{s_i \in E | s_{i;t+l-1} = a_{k_l}, \quad l = 1, \dots, n\}. \tag{10}$$

The symbol sequence $w = (a_{i_1}, \dots, a_{i_n}) \in \{0,1\}^n$ is called an *n-word*, where $\{0,1\}^n$ denotes the set $\{0,1\}^{n-1} \times \{0,1\}$ of *n*-tuples of symbols. This definition was introduced by Mc-Millan [48]. For an instructive example see [5].

Now let us introduce a measure of cylinder sets. For finite sets a measure is provided by the set theoretic cardinality function '#($\cdot$)'. A probability measure for cylinder sets can be defined by

$$p(a_{k_1}, \dots, a_{k_n} | t) = \frac{\#([a_{k_1}, \dots, a_{k_n}]_t)}{N}. \tag{11}$$

Considering all cylinders of given length n at given time t together, we call the corresponding distribution $\{([a_{k_1}, \dots, a_{k_n}]_t, p(a_{k_1}, \dots, a_{k_n} | t)) | t, n \text{ fixed}\}$ *word statistics* of order n. The word statistics can be characterized by measures of complexity, such as Shannon and Rényi entropy [49,50] or, e.g., machine complexity and renormalized entropy [47,51].

The Shannon entropies [49] of order n at time t of the ensemble E are given by

$$H_n(t) = - \sum_{(a_{k_1}, \dots, a_{k_n})} p(a_{k_1}, \dots, a_{k_n} | t)$$
$$\times \log p(a_{k_1}, \dots, a_{k_n} | t). \tag{12}$$

The quantities

$$H(t) = \frac{H_n(t)}{n} \tag{13}$$

measure the information per letter and are called *relative entropies*. The quantities

$$I_{n;q}(t) = \frac{1}{1-q} \log \sum_{(a_{k_1}, \dots, a_{k_n})} p(a_{k_1}, \dots, a_{k_n} | t)^q \tag{14}$$

are called *n*-order *Rényi entropies* depending on the parameter q [50]. The base of the logarithm in the formulas above is arbitrary. But it is recommended to use the $\log_I$, where I is the cardinality of the letter alphabet, because relative entropies will always be normalized to the range [0,1]. In case of a binary encoding ($I=2$) information is measured in binary digits (*bits*) by using the *logarithmus dualis* ld$\equiv$log$_2$. Entropy is a measure of uncertainty of a given probability distribution. It reaches its maximum value $+1$ for uniformly distributed events. It takes its minimum 0 if there is only one certain event with probability 1. For uniform distributions all q-Rényi entropies have the same value $+1$. But for nonuniform distributions the q-Rényi entropies differ significantly. For $q>1$ high word probabilities are enhanced, whereas small probabilities are suppressed. Hence nonuniform distributions can be deformed toward a distribution where only few events are considerably probable by choosing large q

values. The limit of the Rényi entropy for $q \rightarrow 1$ is given by the Shannon entropy due to the rule of L'Hospital. We therefore refer to the Shannon entropy as the $q=1$-Rényi entropy.

III. SIGNALS WITH ADDITIVE NOISE

In this section we are dealing with stochastic processes of the form of Eq. (1). In order to prove the equivalence of symbolic dynamics and spectral approaches [Eqs. 2–4], we assume that the deterministic signal $s(t)$ is provided by a linear harmonic oscillator, while the noise ξ_σ should be regarded as Gaussian white noise with zero mean, variance σ^2, and probability density function $\rho_\xi(x)$ [57]. Under these assumptions Eq. (1) receives the form

$$x(t) = A \sin(\omega t) + \xi_\sigma(t), \tag{15}$$

where A is the amplitude of the harmonic oscillation and the phase offset has been set to zero.

By computing the SNR according to Eq. (2), we obtain

$$Q = \frac{A}{\sigma\sqrt{2}}. \tag{16}$$

This quantity assumes values between zero ($A=0$: there is no signal at all) and plus infinity ($\sigma=0$: there is no additive noise).

A. Static encoding

Now we are going to apply the theoretical concepts mentioned above to the process of Eq. (15), $x(t) = A \sin(\omega t) + \xi_\sigma(t)$. A static encoding can be obtained straightforwardly by choosing $\theta=0$ for all trials. For $Q=0$ (pure white Gaussian noise) $\theta=0$ agrees with the median of the distribution leading to maximal entropy [5,41]. This choice corresponds to the generating partition of a chaotic dynamical system [45,52]. Figure 1 visualizes the symbol matrix Eq. (8), [respectively the ensemble Eq. (9)] of a statically encoded ensemble of $N=100$ epochs of the stochastic process [Eq. (15)] with a SNR $Q=0.5$. In this plot a black pixel denotes the letter "0" while a white pixel denotes the symbol "1."

The symbolic dynamics of the process Eq. (15) can be treated analytically. The probability of observing the symbol "0" at time t, i.e., the measure of the cylinder $[0]_t$, is simply given by

$$p_0(t) = p(0 | t) = \int_{-\infty}^0 \rho_\xi(x - A \sin(\omega t)) dx. \tag{17}$$

After a substitution, this probability can be expressed by the distribution function $F_\xi(x) = \int_{-\infty}^x \rho_\xi(y) \, dy$ as

$$p_0(t) = F_\xi(-A \sin(\omega t)) = \frac{1}{2} \text{erfc}(Q \sin(\omega t)), \tag{18}$$

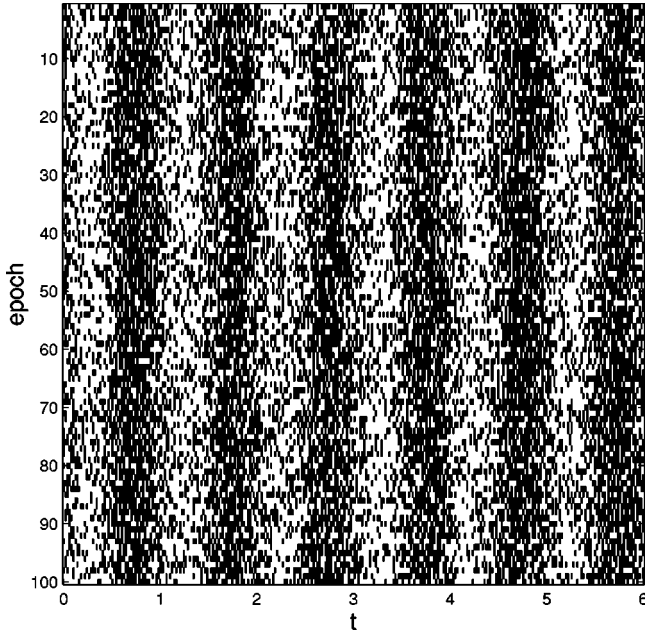where erfc is the complementary error function [53] defined by

FIG. 1. Symbolic dynamics of a simply statically encoded ensemble of $N = 100$ realizations of the stochastic process [Eq. (15)] with a SNR $Q = 0.5$, $\omega = 2\pi$. Black areas denote ''0,'' and white ''1.''

$$\text{erfc}\, x = \frac{2}{\sqrt{\pi}} \int_x^{\infty} e^{-y^2} dy. \qquad (19)$$

Figure 2 shows the one-word Rényi entropy $I_{1;q}(t)$ [Eq. (14)] for different q values. Note that the entropy becomes smaller when $q > 1$ for small $p_0(t)$.

Now we come to the main issue of this section. We suggest an estimator of the signal-to-noise ratio by means of symbolic dynamics. In order to achieve this, we first introduce the time averages of the entropies:
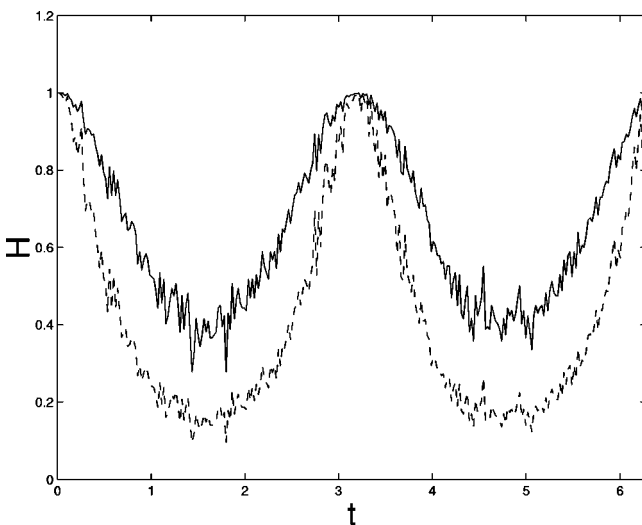
FIG. 2. Running one-word Rényi entropy $I_{1;q}(t)$ [Eq. (14)] of the stochastic process [Eq. (15)] with different q values for an ensemble of $N = 500$ simulated realizations with a SNR $Q = 1$, $\omega = 1$. Solid line: $q = 1$ (Shannon entropy). Dashed line: $q = 4$.

$$J_{n;q} = \frac{1}{T} \int_0^T I_{n;q}(t) dt. \qquad (20)$$

From these averages we compute the quantity

$$S = G\left(\frac{1}{J} - 1\right), \qquad (21)$$

where G is some positive constant to be determined later on. The indices n and q will be omitted subsequently for the sake of convenience. The quantity S can be regarded being a function of the SNR Q of the process of Eq. (15). It is easy to verify that $S(Q) = 0$ for $Q \to 0$, while $S(Q) \to \infty$ for $Q \to \infty$, since J is restricted to the unit interval $0 \leq J \leq 1$. However, we shall prove a stronger claim. That is, $S(Q)$ is asymptotically equivalent to the SNR Q for $n = 1$ and $q = 1$, i.e., $S(Q)$ obtained by the one-word Shannon entropy is a good estimator of the SNR Q. For a proof, see Appendix A.

The following figures show the agreement of $S(Q)$ obtained from an analytical calculation compared to that obtained with numerical results. Additionally, we consider the derivative dS/dQ as an *improvement factor*. Given a process [Eq. (15)] with a SNR Q, we look at the change of $S(Q)$ by slightly altering Q to $Q + \Delta Q$. Then the change of S is given by $\Delta S = (dS/dQ) \Delta Q$. For Q values with $dS(Q)/dQ > 1$, the SNR of the symbolic dynamics can be improved by increasing Q moderately. Figure 3(a) shows the estimate $S(Q)$ depending on Q of the one-word Shannon entropy, while Fig. 3(b) presents the improvement factor. An improvement in the SNR is achieved for $Q \geq 1.6$. This maximum of the SNR improvement factor can be seen as a stochastic resonance phenomenon, as we discussed in Sec. I.

Next we show that using the Rényi entropies for $q > 1$ leads to a further improvement of SNR by symbolic dynamics, because, as we had mentioned above, large q values entail lower entropy values (see Fig. 2). Thus the SNR estimator $S(Q_1)$, obtained by a $q > 1$-Rényi entropy from Eq. (15) with SNR Q_1, agrees with the SNR estimator $S(Q_2)$ given by the Shannon entropy ($q = 1$) from a process with SNR Q_2, where $Q_2 > Q_1$. Figure 4(a) presents analytical (dotted line) as well as numerical results (solid line) of $S(Q)$ for a parameter setting $q = 8$. Figure 4(b) demonstrates that the SNR improvement factor is greater than one for $Q \geq 0.6$.

Finally, we compare the effects of changing the q-parameter with those of changing the word length n. Figure 5(a) presents the numerical estimates of $S(Q)$ for $q = 1$ (solid line), $q = 2$ (dashed line), and $q = 8$ (dotted line). In Fig. 5(b) we demonstrate that changing the order of the word statistics does not provide a considerable improvement of the SNR. Here we plotted the results of the numerical estimates of $S(Q)$ for $n = 1$ (solid line), $n = 2$ (dashed line), and $n = 8$ (dotted line). All functions have been determined for $q = 1$, i.e., for Shannon entropies.

B. Half wave encoding

In Sec. III A we demonstrated that symbolic dynamics provides a good estimator of the SNR of a noisy time series. This estimator depends on two parameters: the word length n
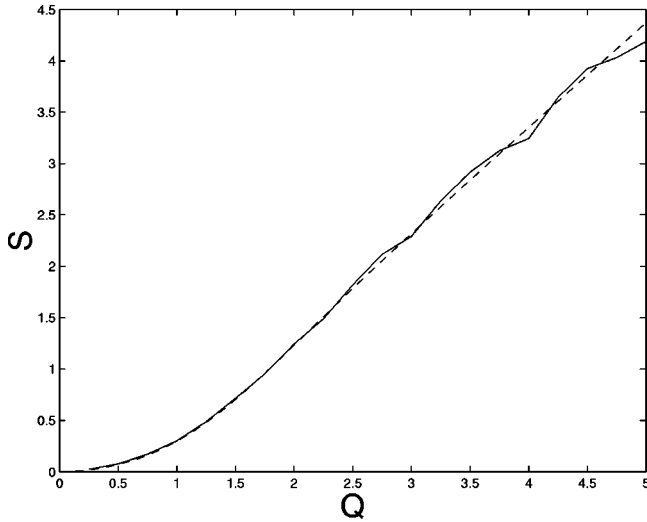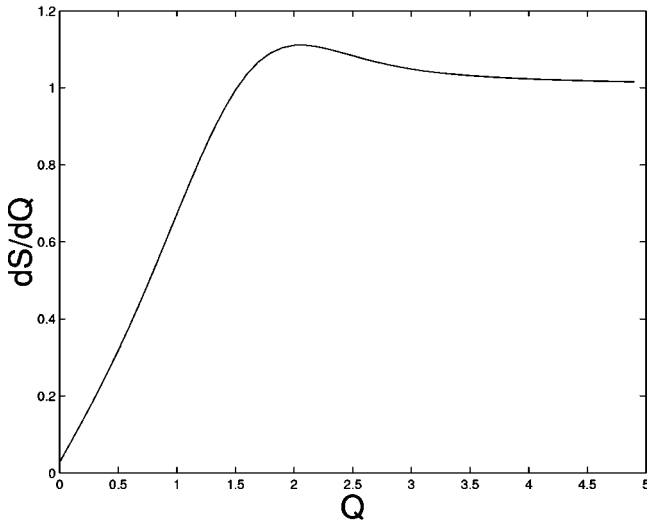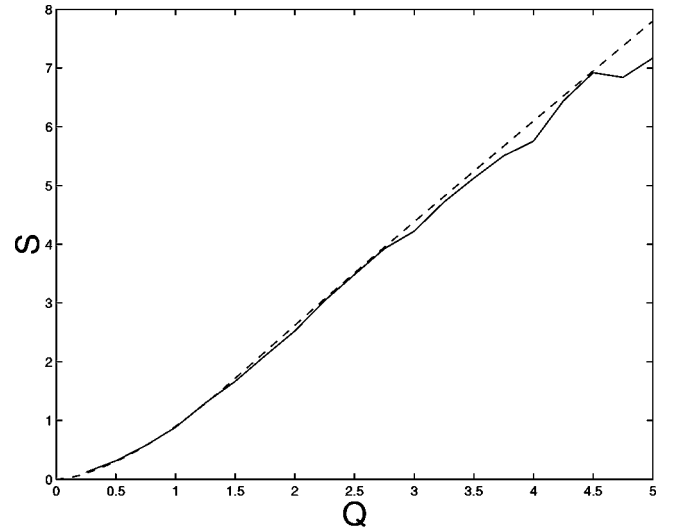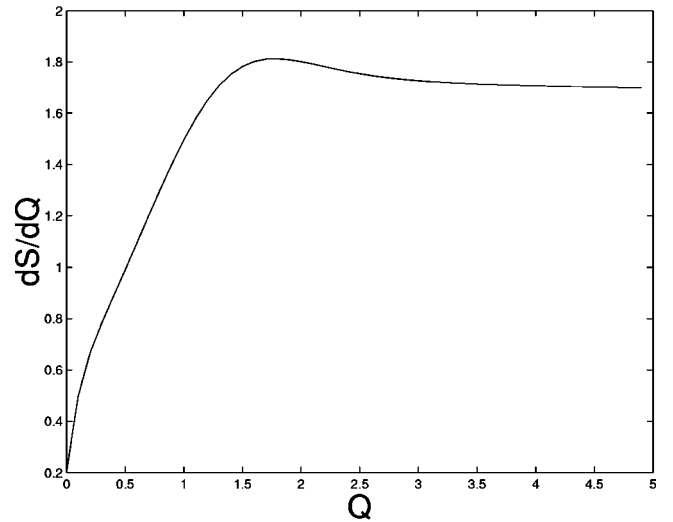
FIG. 3. Estimates of the SNR from symbolic dynamics S depending on the SNR Q of the stochastic process [Eq. (15)] given by the time averaged Shannon entropy [Eq. (21)]. (a) $S(Q)$ from numerical simulations of $N=100$ realizations (solid line) against the analytical result (dashed line). (b) Derivation dS/dQ of the analytical result.

FIG. 4. Estimates of the SNR from symbolic dynamics S depending on the SNR Q of the stochastic process [Eq. (15)] given by the time averaged $q=8$-Rényi entropy [Eq. (21)]. (a) $S(Q)$ from numerical simulations of $N=100$ realizations (solid line) against the analytical result (dashed line). (b) Derivation dS/dQ of the analytical result.

and the Rényi parameter q. We also showed that by tuning q we are able to improve the SNR significantly. This subsection is devoted to a new symbolic encoding technique for further improving the SNR. We employ a method, called *half wave encoding*, that is equivalent to the simple static encoding [Eq. (8)] for a noise-free time series [Eq. (15)] with $\sigma = 0$. This approach rests on the idea of detecting half waves of the signal $x(t)$. A half wave of a sine function is given by an interval between succeeding inflection points. A positive half wave lasts from an inflection point of positive slope to an inflection point of negative slope, while a negative half wave lasts from an inflection point of negative slope to an inflection point of positive slope. Thus, encoding half waves comes out to be equivalent to detecting inflection points. It is well known that inflection points of an analytical function

are points of extremal slope. The conventional way of looking for inflection points is therefore determining the zeros of the second derivative of the function. But in the case of analyzing noisy time series this approach must fail, because computing derivatives of noisy signals numerically enhances the noise. In order to counter this difficulty, we decided to calculate averaged slopes of secants $u(t)$ divided by their variances $v(t)$ within a sliding window of width T_1 (T_1 even) sampling points. We define a *secant slope function* $w(t)$ by

$$u(t) = \frac{1}{T_1} \sum_{k=1}^{T_1/2} \frac{x(t+k) - x(t-k)}{k}, \qquad (22)$$
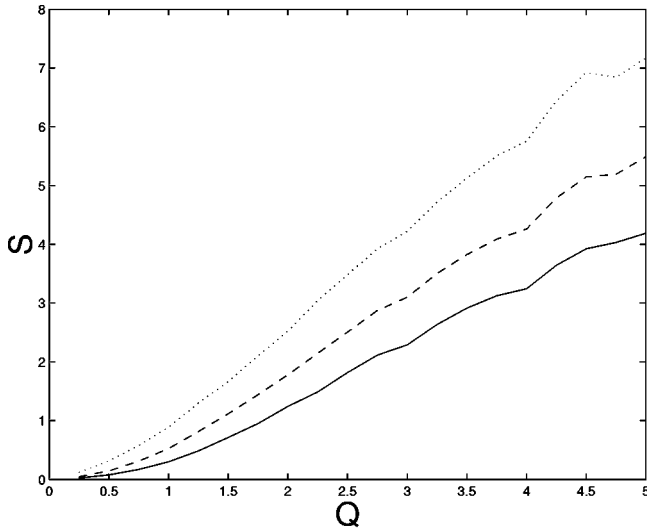
(a)
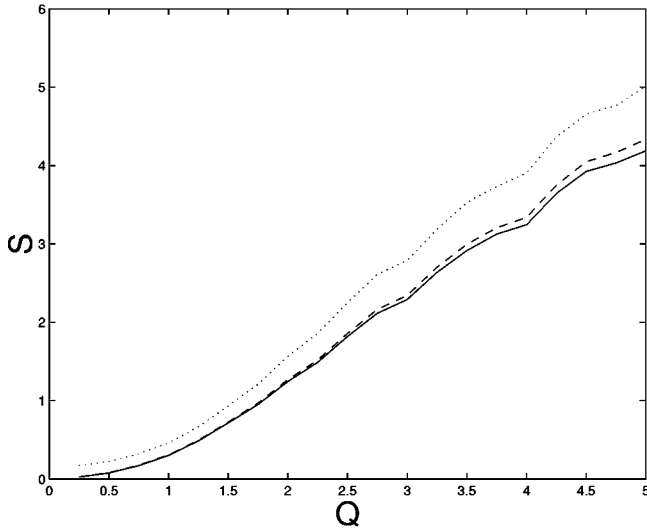
(b)

FIG. 5. Estimates of the SNR from symbolic dynamics S as a function of the SNR Q of the stochastic process [Eq. (15)] given by the time averaged entropies [Eq. (21)] obtained by numerical simulations of an ensemble of $N=100$ statically encoded realizations. (a) $S(Q)$ depending on different Rényi-parameters q. Solid line: $q=1$ (Shannon entropy). Dashed line: $q=2$. Dotted line: $q=8$. (b) $S(Q)$ depending on different word lengths n. Solid line: $n=1$ (symbol statistics). Dashed line: $n=2$. Dotted line: $n=8$.
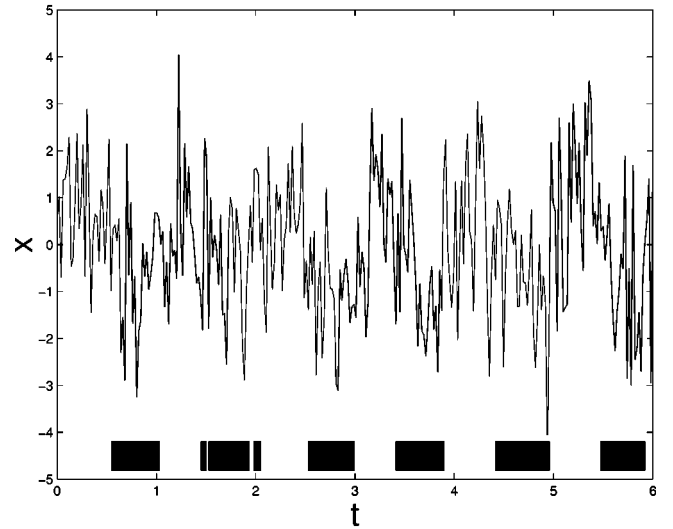
$$v(t) = \frac{1}{T_1-1} \sum_{k=1}^{T_1/2} \left[\frac{x(t)-x(t-k)}{k} - u(t) \right]^2$$
$$+ \left[\frac{x(t+k)-x(t)}{k} - u(t) \right]^2, \quad (23)$$

$$w(t) = \frac{u(t)}{v(t)}. \quad (24)$$

The function $w(t)$ is extremal at the inflection points of $x(t)$, where $u(t)$ also reaches its extrema, while $v(t)$ becomes
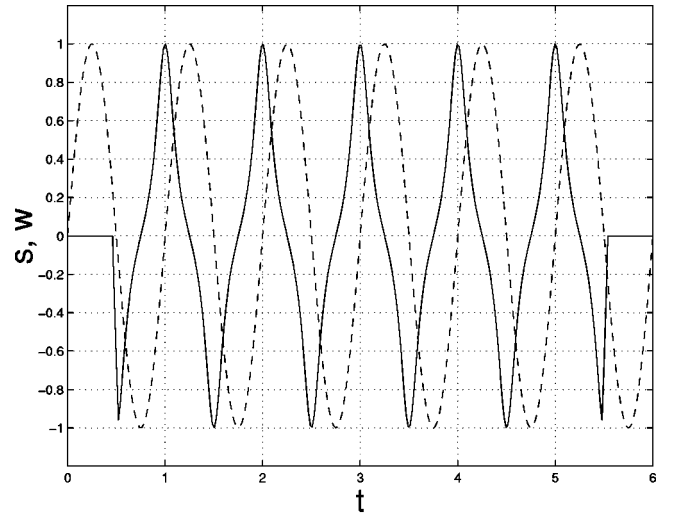
(a)

(b)

FIG. 6. Illustration of the half wave encoding algorithm applied on a pure sine wave and on one realization of the stochastic process [Eq. (15)] with a SNR $Q=0.5$, $\omega=2\pi$. (a) Solid line: ratio of averaged secant slopes by their variances, the *secant slope function* [Eq. (24)], normalized to the maximum of this ratio computed within a running window. The width of the window T_1 is the period T of the sine wave (dashed line). The maxima of the computed ratio correspond to the inflection points of the sine wave having positive slopes. The minima of the ratio correspond to the inflection points of the sine wave with negative slopes. Intervals between the maxima and minima of the ratio correspond to half waves of the original sine wave. (b) One realization of the stochastic process [Eq. (15)] with a SNR $Q=0.5$. Inset: This realization symbolically encoded by the half wave encoding algorithm using a slope averaging window with $T_1=50=T$, a smoothing window with $T_2=25$, and a look ahead for the dynamic encoding of the secant slope function of $l=4$. Black areas denote ''0,'' and white ''1.''

minimal. In contrast, $w(t)$ is minimal at the extrema of $x(t)$, because $u(t)$ is almost zero due to the symmetry of the averaging window where $x(t+k)=x(t-k)$ for the pure sine wave, while $v(t)$ is maximal. Figure 6(a) illustrates the al-
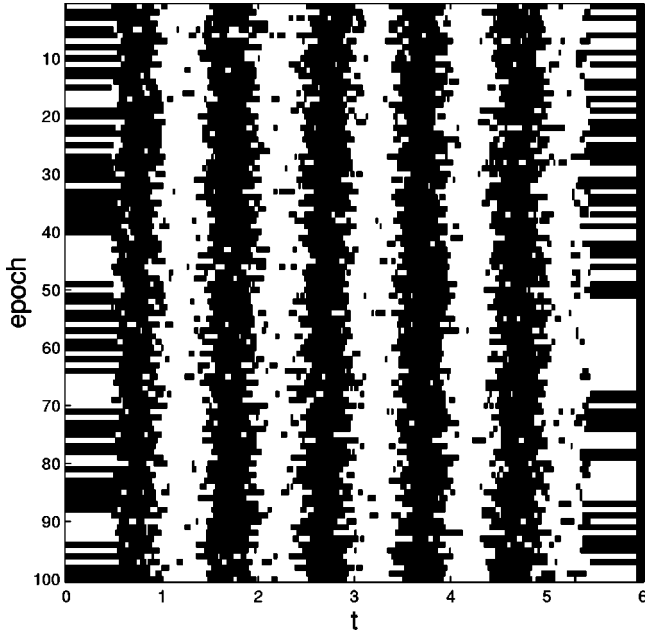
FIG. 7. Symbolic dynamics of the half wave encoded data set from Fig. 1 with parameters $T_1 = 74 \approx T$, $T_2 = 21$, and $l = 4$. The horizontal stripes at the beginning and end of the sequences are artifacts of the sliding window. Black areas denote ''0,'' and white ''1.''

gorithm for a sine wave $x(t) = \sin t$ and its secant slope function $w(t)$. Because of the presence of noise, it is recommended to smooth the secant slope function $w(t)$ by a running averaging algorithm within a window of width T_2 (T_2 odd). This yields a function

$$\bar{w}(t) = \frac{1}{T_2} \sum_{k=-(T_2-1)/2}^{(T_2-1)/2} w(t+k). \qquad (25)$$

For obtaining a symbolic encoding of $x(t)$ one has to determine the monotonic branches of $\bar{w}(t)$. Where $\bar{w}(t)$ is monotonically decreasing from a maximum down to a minimum, we find the positive half waves of $x(t)$. Correspondingly, where $\bar{w}(t)$ is monotonically increasing from a minimum up to a maximum we find the negative half waves of $x(t)$. Monotonicity can be tested by looking a few sampling points l ahead. When $\bar{w}(t+l) > \bar{w}(t)$, the function can be considered to be monotonically decreasing. We assign a symbol ''1'' to the time point t when this holds. Otherwise, we assign the symbol ''0'' if $\bar{w}(t+l) < \bar{w}(t)$, i.e., when $\bar{w}(t)$ is monotonically increasing. This kind of symbolic encoding is a type of *dynamic encoding* [47]. By encoding the smoothed secant slope function $\bar{w}(t)$ of the time series $x(t)$ dynamically, we obtain a half wave encoding of $x(t)$. This is shown in Fig. 6. Figure 6(b) presents a realization of the process of Eq. (15), and the half wave encoding of this realization.

In Fig. 7 we present the half wave encoding of the same ensemble that has been encoded statically in Fig. 1. The half wave encoding has several advantages over other filtering
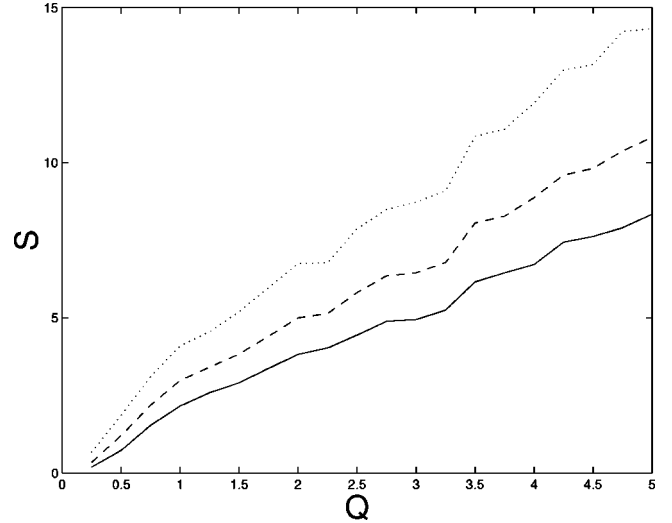

FIG. 8. Estimates of the SNR from symbolic dynamics S as a function of the SNR Q of the stochastic process [Eq. (15)] given by the time averaged entropies [Eq. (21)] obtained by numerical simulations of an ensemble of $N = 100$ realizations that have been encoded using the half wave technique. $S(Q)$ depending on different Rényi parameters q. Solid line: $q = 1$ (Shannon entropy). Dashed line: $q = 2$. Dotted line: $q = 8$.

techniques such as band pass filters. It can be applied to very short time series of at least one and a half periods of the prominent oscillation, while filtering theoretically requires signals having infinite durations in time. The encoding is robust against nonstationarities such as drifts of the signal. It resembles a Poincaré mapping of the system's trajectory but without destroying its time structure, since the detection of inflection points defines a Poincaré section of the state space of the system. Time intervals between the inflection points are not neglected but filled with symbols of one kind, not respecting the noisy dynamics between them. By appropriately choosing the parameters T_1, T_2, and l, one is able to extract certain time scales of the signal.

In Fig. 8 we show the estimates of the SNR by Eq. (21) for the Shannon and for the $q = 2$ and $q = 8$ Rényi entropies of the numerical calculation. As above, the higher order Rényi entropies entail better SNR estimates than the Shannon entropy. On the other hand, a comparison with Fig. 5(a) manifests that the half wave encoding provides better estimates even for the Shannon entropy. Estimating the global slopes of the $S(Q)$ function yields $\Delta S/\Delta Q \approx 4/5$ for the static encoding and $\Delta S/\Delta Q \approx 8/5$ for the half wave encoding, i.e., a doubling of the SNR.

IV. SIGNALS WITH LATENCY NOISE

In this section we are going to describe the problem of randomly distributed phase values, or, in the terminology of ERP research, the problem of latency jitter [Eq. (7)]. Let us specify Eq. (7) by the model

$$x(t) = A \sin(\omega t + \tau), \qquad (26)$$

where τ should be assumed to be an uniformly distributed random variable with zero mean and variance $\sigma^2 = a^2/3$, $a > 0$ with a probability density function ρ_τ obeying

$$\rho_\tau(\tau) = \begin{cases} \dfrac{1}{2a}: & \tau \in [-a, a] \\ \\ 0: & \tau \notin [-a, a] \end{cases} \tag{27}$$

for the sake of simplicity.

A. Determining the damping

It is clear that latency noise smears out the ensemble averages of Eq. (26), thus leading to a deterioration of the SNR. For a qualitative assessment, see Ref. [5]. In order to supply an exact calculation for the latency jitter we first have to transform the distribution of latency times ρ_τ into a distribution of signal values ρ_x. This can be done using a Frobenius-Perron equation [54]

$$\rho_x(x) = \int_{-\infty}^{\infty} d\tau\, \rho_\tau(\tau)\, \delta(x - \sin(t + \tau)) \tag{28}$$

by restricting ourselves to the case where $A = 1$ and $\omega = 1$ without loss of generality. Here we have to discriminate

three different cases for the noise level: (i) $a < \pi/2$, (ii) $\pi/2 \leq a < \pi$, and (iii) the latency jitter is so large that $x(t)$ ranges between -1 and $+1$ for all times t. That is, $a \geq \pi$.

The power of the jittering signal $x(t)$ [Eq. (26)] is smaller than the rms of the pure sine wave $\sin t$, $1/\sqrt{2}$. We therefore introduce a quantity measuring the effect of latency noise, called a *damping factor*, by defining

$$D = \sqrt{2P_x}. \tag{29}$$

This quantity is the analogue to the SNR Q defined in Eq. (2) for latency noise. For a process mixing Eqs. 15 and 26 the SNR is given by $Q = (AD)/(\sigma\sqrt{2})$. The power P_x is given by

$$P_x = \frac{1}{T} \int_0^T \bar{x}^2(t)\, dt \tag{30}$$

due to Eq. (3) where $\bar{x}(t)$ is the ensemble average of $x(t)$.

For the three cases of different noise levels we obtain

$$D = \begin{cases} \sqrt{\dfrac{(\pi^2 + 4a(\pi - a))(\cos(4a) - 1)(4a(\pi^2 - 4a^2))(\mathrm{Si}(4a) - \mathrm{Si}(2\pi) - \mathrm{Si}(4a - 2\pi) + \mathrm{Si}(4a + 2\pi))}{2(a\pi^3 - 4a^3\pi)}}: & a < \dfrac{\pi}{2} \\ \\ \sqrt{\dfrac{\sin^2 a - \mathrm{Si}(2a) + \mathrm{Si}(2\pi)}{\pi a}}: & \dfrac{\pi}{2} \leq a < \pi \\ \\ 0: & a \geq \pi \end{cases} \tag{31}$$

Here Si refers to the sine integral:

$$\mathrm{Si}\, x = \int_0^x \frac{\sin t}{t}\, dt. \tag{32}$$

A graph of the dependence of D on the noise intensity $a = \sigma\sqrt{3}$ is shown in Fig. 9. For a derivation of Eq. (31), see Appendix B.

B. Static encoding

We come now to the symbolic dynamics of the latency jitter (Fig. 10). It is rather obvious that the probability of the symbol ''0'' of a pure sine wave $A \sin t$ is given by a step function

$$p_0(t) = \begin{cases} 0: & 0 \leq t < \pi \\ 1: & \pi \leq t < 2\pi \end{cases} \tag{33}$$

modulo 2π. In order to obtain the probability $\tilde{p}_0(t)$ in the case of latency noise one has to compute the convolution of $p_0(t)$ with the probability density function ρ_τ of the jitter τ [5]:

$$\tilde{p}_0(t) = \int_{-\infty}^{\infty} p_0(t - t')\, \rho_\tau(t')\, dt'. \tag{34}$$

Inserting Eq. (27) into Eq. (34) yields

$$\tilde{p}_0(t) = \frac{1}{2a} \int_{t-a}^{t+a} p_0(u)\, du. \tag{35}$$

As above, we have to consider three different cases: (i) $a < \pi/2$, (ii) $\pi/2 \leq a < \pi$, and (iii) $a \geq \pi$. In case (iii) we simply obtain the constant function $\tilde{p}_0(t) = 1/2$. For cases (i) and (ii) the symbol probabilities are piecewise linear functions

$$\tilde{p}_0(t) = \begin{cases} \dfrac{a - t}{2a}: & -a \leq t < a \\ \\ 0: & a \leq t < \pi - a \\ \\ \dfrac{a + t - \pi}{2a}: & \pi - a \leq t < a + \pi \\ \\ 1: & a + \pi \leq t < 2\pi - a \end{cases} \tag{36}$$
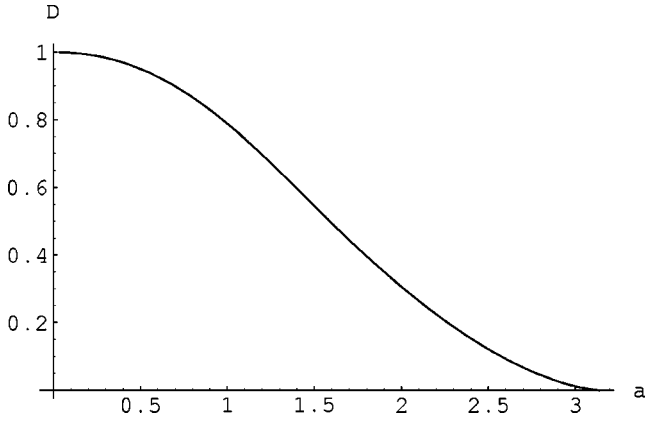
for $a < \pi/2$, and

FIG. 9. Damping D [Eq. (31)] of the stochastic process [Eq. (7)] as a function of latency jitter a.

$$\widetilde{p}_0(t) = \begin{cases} \dfrac{a-t}{2a}: & -\pi+a \leq t < \pi-a \\[2ex] 1-\dfrac{\pi}{2a}: & \pi-a \leq t < a \\[2ex] \dfrac{a+t-\pi}{2a}: & a \leq t < 2\pi-a \\[2ex] \dfrac{\pi}{2a}: & 2\pi-a \leq t < \pi+a \end{cases} \qquad (37)$$

for $\pi/2 \leq a < \pi$.

Our remaining job is to apply our theory of the SNR to this model. To this end we supply the word probabilities $\widetilde{p}_0(t)$ and $1-\widetilde{p}_0(t)$ into Eqs. 12 and 14 in order to compute Shannon and Rényi entropies and finally the SNR estimate S
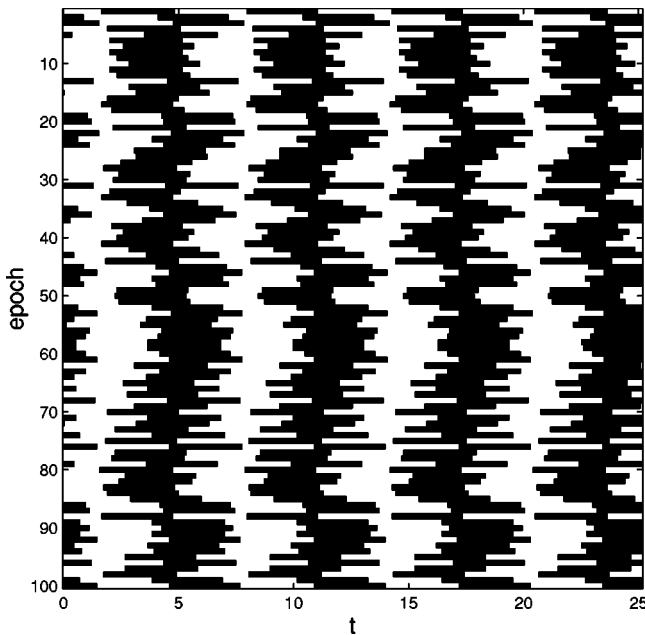

FIG. 10. Symbolic dynamics of a statically encoded ensemble of $N=100$ realizations of the stochastic process [Eq. (26)] ($\omega=1$) for latency jitter $a=\pi/2$. Black areas denote ''0,'' and white ''1.''
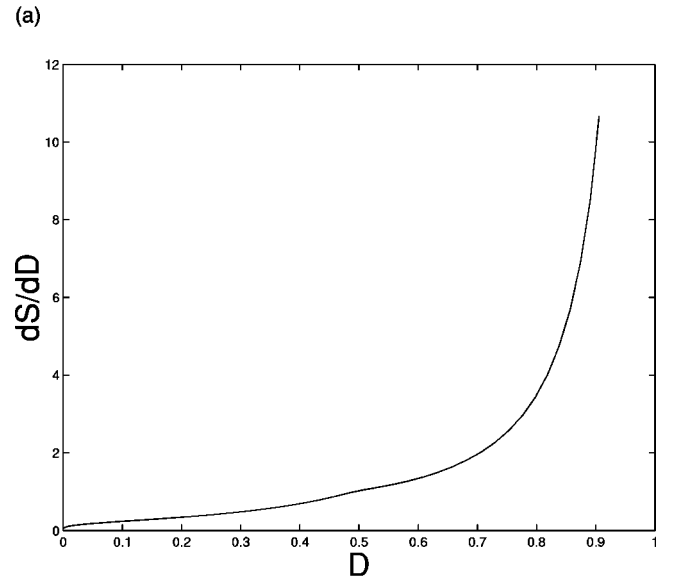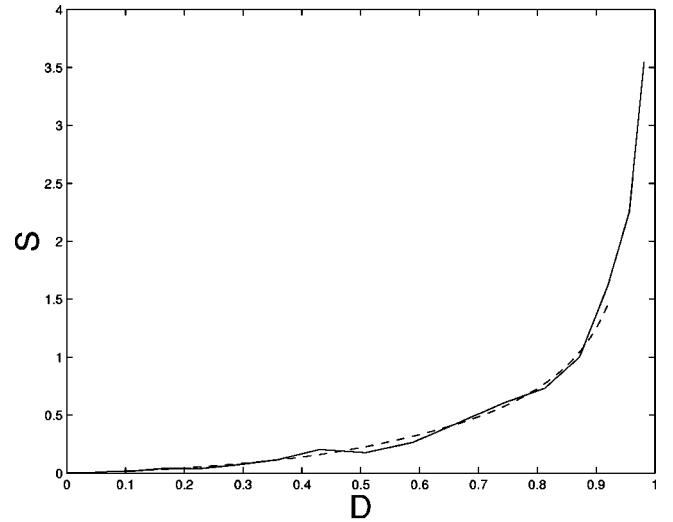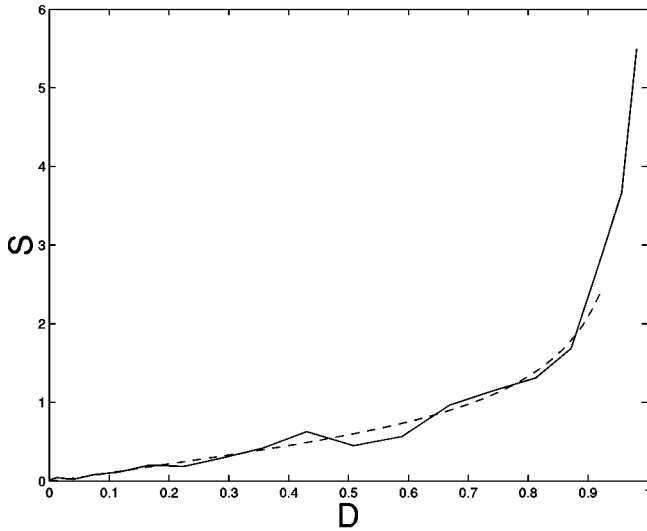

(a)

(b)

FIG. 11. Estimates of the SNR from symbolic dynamics S depending on the damping D of the stochastic process [Eq. (26)] given by the time averaged Shannon entropy [Eq. (21)]. (a) $S(D)$ from numerical simulations of $N=100$ realizations (solid line) against the analytical result (dashed line). (b) Derivation dS/dD of the analytical result.

by Eq. (21), now depending on the damping D instead of the SNR Q. The next figures present the results of analytical and numerical calculations. Above we show the functions $S(D)$ of the analytical issue (dotted line) and for the numerical simulations (solid line). Below, we present the derivatives dS/dD as the SNR improvement factor. Figure 11 provides $S(D)$ and dS/dD computed from the Shannon entropy of the symbol distribution. The improvement factor reaches 1 for $D \geq 0.51$.

By increasing the q-parameter of the Rényi entropy we are able to boost the SNR improvement factor. Figure 12 shows the functions $S(D)$ and dS/dD for $q=8$. Improvement of the SNR is obtained at $D \geq 0.02$.

Finally, we present results from the numerical computation of higher order word statistics. Figure 13(a) repeats the

(a)

(b)

FIG. 12. Estimates of the SNR from symbolic dynamics S depending on the damping D of the stochastic process [Eq. (26)] given by the time averaged $q=8$-Rényi entropy [Eq. (21)]. (a) $S(D)$ from numerical simulations of $N=100$ realizations (solid line) against the analytical result (dashed line). (b) Derivation dS/dD of the analytical result.
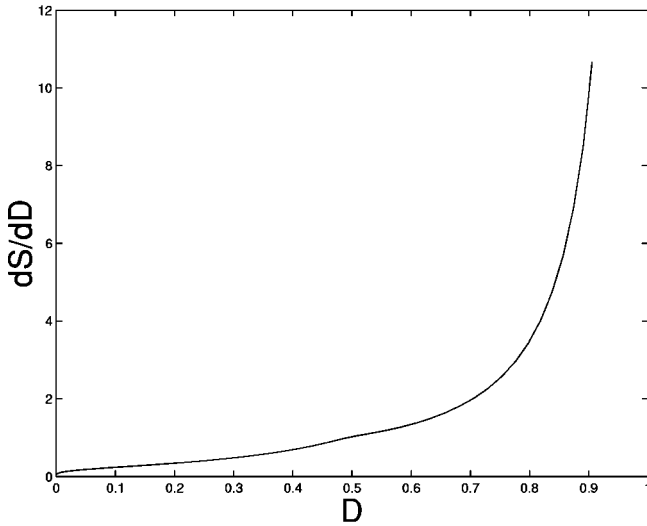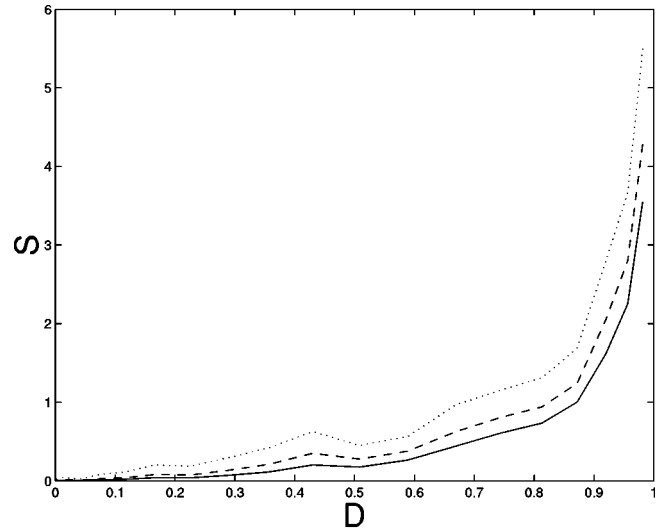

(a)

(b)

FIG. 13. Estimates of the SNR from symbolic dynamics S as a function of the damping D of the stochastic process [Eq. (26)] given by the time averaged entropies [Eq. (21)] obtained by numerical simulations of an ensemble of $N=100$ statically encoded realizations. $S(D)$ depending on different Rényi parameters q. Solid line: $q=1$ (Shannon entropy). Dashed line: $q=2$. Dotted line: $q=8$. (b) $S(D)$ depending on different word lengths n. Solid line: $n=1$ (symbol statistics). Dashed line: $n=2$. Dotted line: $n=8$.
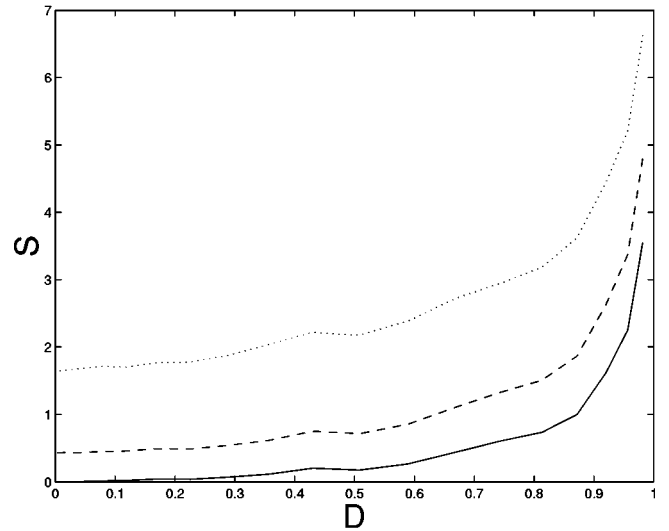
$S(D)$ curves for different q-parameters, while Fig. 13(b) shows the effect of using longer words. It is easy to recognize that going from symbol statistics (solid line) to word lengths $n=2$ (dashed line), and $n=8$ (dotted line) entails better SNR estimates. Thus symbolic dynamics of higher order word statistics is able to capture and diminish latency noise.

V. DISCUSSION

In this paper we studied the requirements of traditional ERP analysis by means of symbolic dynamics. We discussed two kinds of model systems. In the first one, an ensemble of harmonic oscillators provides sine waves of a certain ampli-

tude, all starting with the same initial conditions yielding the same phase offset of zero. These deterministic signals are subsequently corrupted by white Gaussian noise of a given dispersion. In the second model, an ensemble of harmonic oscillators provides sine waves of a certain amplitude as before but starting at different, randomly distributed, initial conditions obeying an uniform distribution of a given variance. This yields an ensemble of sine waves with randomly distributed phase offsets. The SNR of the first model is simply given by Eq. (2). We introduced the symbolic dynamics of this model by a binary static encoding corresponding to a partition of the system's state space into two cells. From the

distributions of the symbols we obtain time dependent measures of complexity such as Shannon and higher order Rényi entropies. The time average of the Shannon entropy of one-word cylinders yields a good estimator of the SNR. We defined a SNR improvement factor by the derivative of the estimator with respect to the linear SNR, and found that there is a maximum of the improvement factor at intermediate noise levels. This maximum might be related to the phenomenon of stochastic resonance known from threshold devices. We shall address this issue more thoroughly in a forthcoming paper.

We have shown that by using higher order Rényi entropies we are able to shift the maximum of the SNR improvement factor toward lower noise amplitudes, and hence improve the SNR by symbolic dynamics. A further improvement of SNR is obtained by an encoding strategy called half wave encoding. This encoding scheme is equivalent to simple static encoding for pure sine waves. For stochastic processes mixed of sine waves and additive noise the half wave encoding detects the inflection points of the deterministic signal, and fills the time intervals between them up with symbols of one kind, e.g., with 0's for negative half waves of the underlying sine function and with 1's for the positive half waves. Detecting inflection points is a kind of Poincaré mapping. It can be used for determining a time series consisting of time intervals [55]. But this procedure spoils information about the absolute timing. Our half wave encoding technique keeps this information by generating sequences of only 1's and 0's, and neglecting the noisy behavior between the inflection points, thus increasing the SNR. The half wave encoding is furthermore insensitive against linear or slowly nonlinear drifts of the time series because it is founded on computing approximated first derivatives of the signals. It can also be applied to ensembles of short time series, whereas linear filter techniques theoretically demand signals of infinite duration.

With the second model of deterministic signals with noisy phases we studied the impact of the phase distribution on the SNR by defining a damping factor. The SNR estimator given by the symbolic dynamics comes out to be a monotonically increasing function of the damping. We obtain an improvement of SNR by symbolic dynamics by considering higher words statistics. Thus we have demonstrated that even if the prerequisites of the traditional approach of ERP analysis were fulfilled symbolic dynamics would yield better results with respect to the signal-to-noise ratio.

APPENDIX A: PROOF OF THE ASYMPTOTIC EQUIVALENCE OF S AND Q

The assertion states that

$$\lim_{Q\to\infty} \frac{S(Q)}{Q} = 1.\qquad (A1)$$

Hence we first have to prove that the ratio $S(Q)/Q$ converges for $Q\to\infty$, and then we have to demonstrate that the limit is equal to 1. In order to achieve the first part of the proof, we show that $S(Q)/Q$ is both monotonically increasing and bounded from above. Monotonicity can be demonstrated by considering the first derivative of the function $S(Q)/Q$. By Eq. (21) we obtain

$$\left(\frac{S(Q)}{Q}\right)' = G\left(1 - \frac{1}{J} - Q\frac{J'}{J^2}\right).\qquad (A2)$$

The derivative of $J(Q)$ is given by

$$J' = -\frac{1}{2\pi^{3/2}}\int_0^{2\pi} \sin t\, \exp(-Q^2\sin^2 t)$$
$$\times \mathrm{ld}\left[\frac{\mathrm{erfc}(-Q\sin t)}{\mathrm{erfc}(Q\sin t)}\right] dt,\qquad (A3)$$

where we integrate over one period of the signal $x(t)$. For the sake of convenience we let the frequency $\omega = 1$. It follows from the symmetry and monotonicity of the complementary error function [53] and from the properties of the sine function that the integrand is non-negative over the whole interval $[0, 2\pi]$. Therefore, J' is negative for all Q (recall, that $Q \geq 0$). We conclude that

$$\left(\frac{S(Q)}{Q}\right)' = G\left(1 - \frac{1}{J} - Q\frac{J'}{J^2}\right) > 0.\qquad (A4)$$

Thus $S(Q)/Q$ is strongly monotonically increasing.

Proving boundedness is a bit more complicated. For this aim we shall first approximate the probability $p_0(t)$ by a step function. Since the one-word entropy [Eq. (12)] is π periodic, it will be enough defining this function only at the interval $[0, \pi]$:

$$p_0^*(t) = \begin{cases} \dfrac{1}{4}: & 0 \leq t < t^* \\[6pt] \varepsilon: & t^* \leq t < \pi - t^* \\[6pt] \dfrac{1}{4}: & \pi - t^* \leq t < \pi. \end{cases}\qquad (A5)$$

For Q large enough, $\varepsilon < 1/4$ is given by $\varepsilon = \mathrm{erfc}(-Q)/2$, while t^* is determined by $p_0^*(t^*) = 1/4$, yielding $t^* = \arcsin(a/Q)$, with $a = \mathrm{erfc}^{-1}(1/2)$ and erfc^{-1} as the inverse complementary error function. From $p_0^*(t)$ we compute the Shannon entropy [Eq. (12)]

$$H^*(t) = \begin{cases} b: & 0 \leq t < t^* \\[4pt] -\varepsilon\, \mathrm{ld}\,\varepsilon - (1-\varepsilon)\mathrm{ld}(1-\varepsilon): & t^* \leq t < \pi - t^* \\[4pt] b: & \pi - t^* \leq t < \pi, \end{cases}$$
$$(A6)$$

where we set $b = 2 - (3\,\mathrm{ld}\,3)/4$. The time average integral of $H^*(t)$ is given by

$$J^* = \frac{1}{\pi} \int_0^\pi H^*(t) dt$$

$$= \frac{2b}{\pi} \arcsin\left(\frac{a}{Q}\right) - \frac{1}{\pi} \arccos\left(\frac{a}{Q}\right)$$

$$\times \left\{ 2[\mathrm{ld}(\mathrm{erfc}(-Q)) - 1] + \mathrm{erfc} Q \, \mathrm{ld}\left[\frac{\mathrm{erfc}(Q)}{\mathrm{erfc}(-Q)}\right] \right\}. \tag{A7}$$

Now we can compute the quantities $S^*(Q) = G(1/J^* - 1)$ and $S^*(Q)/Q = G(1 - J^*)/(QJ^*)$. Because $p_0^*(t) \leqslant p_0(t)$ for all $t \in [0, \pi]$, it holds that $H^*(t) \leqslant H(t)$ and therefore $S^*(Q)/Q > S(Q)/Q$, thus providing an upper boundary of $S(Q)/Q$. By expanding the logarithm and the complementary error function into power series [56], we obtain $\lim_{Q \to \infty} J^* = 0$ and $\lim_{Q \to \infty} QJ^* = 2ab/\pi$, and therefore

$$\lim_{Q \to \infty} \frac{1 - J^*(Q)}{QJ^*(Q)} = \frac{\pi}{2ab}. \tag{A8}$$

Consequently, we have proven that $S(Q)/Q$ has an upper bound, namely, $\pi/(2ab)$ when Q is large enough so that $\varepsilon < 1/4$. Since $S(Q)/Q$ is strongly monotonically increasing as well as bounded from above, it is also convergent. By appropriately choosing the constant G we force the limit $\lim_{Q \to \infty} S(Q)/Q$ to be 1. Then we have shown that $S(Q)/Q$ is asymptotically equivalent to the SNR Q. For practical purpose we estimate the limit numerically as $1/G = \lim_{Q \to \infty}(1 - J(Q))/(QJ(Q)) \approx (1 - J(200))/(200J(200)) = 1.69981$.

APPENDIX B: DERIVATION OF THE DAMPING FACTOR

The Dirac distribution in the integrand of Eq. (28) can be evaluated by the theorem

$$\delta(\varphi(y)) = \sum_{i : \varphi(y_i) = 0} \frac{1}{|\varphi'(y_i)|} \delta(y - y_i), \tag{B1}$$

where y_i are simple zeros of the function φ. The zeros of the function $\varphi(\tau) = x - \sin(t + \tau)$ are given by

$$\tau_{k;1} = 2\pi k + \arcsin x - t, \tag{B2}$$

$$\tau_{k;2} = 2\pi k + \pi - \arcsin x - t, \tag{B3}$$

while the derivative is $\varphi'(\tau) = -\cos(t + \tau)$. The variables t and x are regarded to be parameters, k is an integer ranging from $-\infty$ to ∞. Thus Eq. (B1) leads to

$$\delta(x - \sin(t + \tau)) = \sum_{k = -\infty}^{\infty} \frac{\delta(\tau - \tau_{k;1})}{|\cos(2\pi k + z)|} + \frac{\delta(\tau - \tau_{k;2})}{|\cos(2\pi k + \pi - z)|},$$

where we abbreviated $z = \arcsin x$. By using the periodicity and symmetry of the cosine function, we obtain

$$\delta(x - \sin(t + \tau)) = \frac{1}{|\cos z|} \sum_{k = -\infty}^{\infty} \delta(\tau - \tau_{k;1}) + \delta(\tau - \tau_{k;2}),$$

and finally, by expanding $z = \arcsin x$, we obtain

$$\delta(x - \sin(t + \tau)) = \frac{1}{\sqrt{1 - x^2}} \sum_{k = -\infty}^{\infty} \delta(\tau - \tau_{k;1}) + \delta(\tau - \tau_{k;2}). \tag{B4}$$

Inserting Eq. (B4) and the density [Eq. (27)] into the Frobenius-Perron equation (28) entails

$$\rho_x(x) = \frac{1}{2a\sqrt{1 - x^2}} \int_{-a}^{a} d\tau \sum_{k = -\infty}^{\infty} \delta(\tau - \tau_{k;1}) + \delta(\tau - \tau_{k;2}). \tag{B5}$$

Then we condense the integral into a normalization constant

$$N = \int_{-a}^{a} d\tau \sum_{k = -\infty}^{\infty} \delta(\tau - \tau_{k;1}) + \delta(\tau - \tau_{k;2}).$$

This provides the result

$$\rho_x(x) = \frac{N}{2a\sqrt{1 - x^2}}. \tag{B6}$$

Next we must consider cases (i)–(iii) of the noise level a. Let us first look at case (iii). The constant N_3 must obey the normalization

$$\int_{-1}^{1} \frac{N_3}{2a\sqrt{1 - x^2}} dx = 1. \tag{B7}$$

The integral can be performed by elementary calculus yielding $N_3/(2a) = 1/\pi$. Hence the density ρ_x is given by

$$\rho_x(x) = \frac{1}{\pi\sqrt{1 - x^2}}. \tag{B8}$$

Note that this is exactly the invariant density of the fully chaotic logistic map $x_{n+1} = 1 - 2x_n^2$ [30].

For both the other cases (i) and (ii), the range of dispersion of $x(t)$ depends on the actual time t. The factor N is determined by the constraint

$$\int_{\min[\sin(t-a), \sin(t+a)]}^{\max[\sin(t-a), \sin(t+a)]} \frac{N(t)}{2a\sqrt{1 - x^2}} dx = 1, \tag{B9}$$

and now depends on time.

For case (i) we have to distinguish six branches of the function $N_1(t)$:

$$N_1(t) = \begin{cases} 1: & a - \dfrac{\pi}{2} \le t < \dfrac{\pi}{2} - a \\[2ex] \dfrac{2a}{a - t + \dfrac{\pi}{2}}: & \dfrac{\pi}{2} - a \le t < \dfrac{\pi}{2} \\[3ex] \dfrac{2a}{a + t - \dfrac{\pi}{2}}: & \dfrac{\pi}{2} \le t < a + \dfrac{\pi}{2} \\[3ex] 1: & a + \dfrac{\pi}{2} \le t < \dfrac{3\pi}{2} - a \\[2ex] \dfrac{2a}{a - t + \dfrac{3\pi}{2}}: & \dfrac{3\pi}{2} - a \le t < \dfrac{3\pi}{2} \\[3ex] \dfrac{2a}{a + t - \dfrac{3\pi}{2}}: & \dfrac{3\pi}{2} \le t < a + \dfrac{3\pi}{2}. \end{cases} \tag{B10}$$

Also six branches must be discriminated for case (ii):

$$N_2(t) = \begin{cases} \dfrac{2a}{\pi}: & \dfrac{\pi}{2} - a \le t < a - \dfrac{\pi}{2} \\[3ex] \dfrac{2a}{a - t + \dfrac{\pi}{2}}: & a - \dfrac{\pi}{2} \le t < \dfrac{\pi}{2} \\[3ex] \dfrac{2a}{a + t - \dfrac{\pi}{2}}: & \dfrac{\pi}{2} \le t < \dfrac{3\pi}{2} - a \\[3ex] \dfrac{2a}{\pi}: & \dfrac{3\pi}{2} - a \le t < a + \dfrac{\pi}{2} \\[3ex] \dfrac{2a}{a - t + \dfrac{3\pi}{2}}: & a + \dfrac{\pi}{2} \le t < \dfrac{3\pi}{2} \\[3ex] \dfrac{2a}{a + t - \dfrac{3\pi}{2}}: & \dfrac{3\pi}{2} \le t < \dfrac{5\pi}{2} - a. \end{cases} \tag{B11}$$

From the distribution densities ρ_x obtained by the normalization functions $N_{1;2;3}(t)$ we compute the expectation values

$$\bar{x}(t) = \frac{N(t)}{2a} \int_{\min[\sin(t-a),\sin(t+a)]}^{\max[\sin(t-a),\sin(t+a)]} \frac{x}{\sqrt{1-x^2}} dx,$$

$$\bar{x}(t) = \frac{N(t)}{2a} [\sqrt{1-x^2}]_{\min[\sin(t-a),\sin(t+a)]}^{\max[\sin(t-a),\sin(t+a)]}. \tag{B12}$$

Here we report the result for N_3. In this case, the expectation value is just zero for all time, meaning that a latency jitter of π or larger smears out any signal at all. The other expectation values are functions of time again. These are supplied to the computation of the signal power [Eq. (3)] employing Eq. (30). This integration has to be performed over the six branches of $N_1(t)$ and $N_2(t)$, respectively; but we shall omit these tedious calculations. Finally, we insert Eq. (30) into the definition of the damping factor [Eq. (29)]. This yields Eq. (31).

[1] D. Regan, *Evoked Potentials in Psychology, Sensory, Physiology and Clinical Medicine* (Chapman and Hall, London, 1972).

[2] D. Regan, *Human Brain Electrophysiology: Evoked Potentials and Evoked Magnetic Fields in Science and Medicine* (Elsevier, New York, 1989).

[3] *Electroencephalography. Basic Principles, Clinical Applications, and Related Fields*, 3rd ed., edited by E. Niedermeyer and F.L.D. Silva (Williams and Wilkins, Baltimore, 1993).

[4] B.I. Turetsky, J. Raz, and G. Fein, Electroencephalography Clinical Neurophysiol. **71**, 310 (1988).

[5] P. beim Graben, J.D. Saddy, M. Schlesewsky, and J. Kurths, Phys. Rev. E **62**, 5518 (2000).

[6] A. Papoulis, *Probability, Random Variables, and Stochastic Processes*, 3rd ed. McGraw-Hill Series in Electrical Engineering, Communications and Signal Processing (McGraw-Hill, New York, 1991).

[7] R. Coppola, R. Tabor, and M.S. Buchsbaum, Electroencephalography Clinical Neurophysiol. **44**, 214 (1978).

[8] R.A. Dobie and M.J. Wilson, Electroencephalography Clinical Neurophysiol. **80**, 194 (1991).

[9] A. Puce, S.F. Berkovic, P.J. Cadusch, and P.F. Bladin, Electroencephalography Clinical Neurophysiol. **92**, 352 (1994).

[10] E. Başar, *EEG–Brain Dynamics. Relations between EEG and Brain Evoked Potentials* (Elsevier/North Holland Biomedical Press, Amsterdam, 1980).

[11] J. Möcks, T. Gasser, and P.D. Tuan, Electroencephalography Clinical Neurophysiol. **57**, 571 (1984).

[12] T. Gasser, J. Möcks, and R. Verleger, Electroencephalography Clinical Neurophysiol. **55**, 717 (1983).

[13] E. Courchesne, Electroencephalography Clinical Neurophysiol. **45**, 754 (1978).

[14] B.I. Turetsky, J. Raz, and G. Fein, Psychophysiology **26**, 700 (1989).

[15] S. Krieger, J. Timmer, S. Lis, and H.M. Olbrich, J. Neural Transmission **99**, 103 (1995).

[16] E. Callaway and R.A. Halliday, Electroencephalography Clinical Neurophysiol. **34**, 125 (1973).

[17] R. Benzi, A. Sutera, and A. Vulpiani, J. Phys. A **14**, L453 (1981).

[18] B. McNamara, K. Wiesenfeld, and R. Roy, Phys. Rev. Lett. **60**, 2626 (1988).

[19] L. Gammaitoni, P. Hänggi, P. Jung, and F. Marchesoni, Rev. Mod. Phys. **70**, 223 (1998).

[20] M.M. Alibegov, Phys. Rev. E **59**, 4841 (1999).

[21] L. Gammaitoni, Phys. Rev. E **52**, 4691 (1995).

[22] L. Gammaitoni, Phys. Lett. A **208**, 315 (1995).

[23] J.J. Collins, C.C. Chow, and T.T. Imhoff, Phys. Rev. E **52**, R3321 (1995).

[24] J.J. Collins, C.C. Chow, A.C. Capela, and T.T. Imhoff, Phys. Rev. E **54**, 5575 (1996).

[25] A.R. Bulsara and A. Zador, Phys. Rev. E **54**, R2185 (1996).

[26] B. McNamara and K. Wiesenfeld, Phys. Rev. A **39**, 4854 (1989).

[27] D. Gong, G. Quin, G. Hu, and X. Wen, Phys. Lett. A **159**, 147 (1991).

[28] D. Gong, G. Hu, X. Wen, C. Yang, G. Qin, R. Li, and D. Ding, Phys. Rev. A **46**, 3243 (1992).

[29] D. Gong, G. Hu, X. Wen, C. Yang, G. Qin, R. Li, and D. Ding, Phys. Rev. E **48**, 4862 (1993).

[30] B.-L. Hao, *Elementary Symbolic Dynamics and Chaos in Dissipative Systems* (World Scientific, Singapore, 1989).

[31] B.-L. Hao, Physica D **51**, 161 (1991).

[32] U. Schwarz, A.O. Benz, J. Kurths, and A. Witt, Astron. Astrophys. **277**, 215 (1993).

[33] T. Buchner and J.J. Zebrowski, Phys. Rev. E **60**, 3973 (1999).

[34] L. Flepp, R. Holzner, E. Brun, M. Finardi, and R. Badii, Phys. Rev. Lett. **67**, 2244 (1991).

[35] J. Kurths, A. Voss, A. Witt, P.I. Saparin, H.J. Kleiner, and N. Wessel, Chaos **5**, 88 (1995).

[36] M. Schiek, F.R. Drepper, R. Engbert, H.H. Abel, and K. Suder, in *Nonlinear Analysis of Physiological Data* (Ref. [58]), pp. 191–213.

[37] C. Scheffczyk, A. Zaikin, M. Rosenblum, R. Engbert, R. Krampe, and J. Kurths, Int. J. Bifurcation Chaos Appl. Sci. Eng. **7**, 1441 (1997).

[38] R. Engbert, C. Scheffczyk, R.T. Krampe, M. Rosenblum, J. Kurths, and R. Kliegl, Phys. Rev. E **56**, 5823 (1997).

[39] P. Tass, J. Kurths, M. Rosenblum, G. Guasti, and H. Hefter, Phys. Rev. E **54**, R2224 (1996).

[40] P.I. Saparin, W. Gowin, J. Kurths, and D. Felsenberg, Phys. Rev. E **58**, 6449 (1998).

[41] P.E. Rapp, I.D. Zimmerman, E.P. Vining, N. Cohen, A.M. Albano, and M.A. Jiménez-Montano, J. Neurosci. **14**, 4731 (1994).

[42] K. Mischaikow, M. Mrozek, I. Reiss, and A. Szymczak, Phys. Rev. Lett. **82**, 1144 (1999).

[43] X.Z. Tang and E.R. Tracy, Chaos **8**, 688 (1998).

[44] J.P. Crutchfield and N.H. Packard, Int. J. Theor. Phys. **21**, 434 (1982).

[45] J.P. Crutchfield and N.H. Packard, Physica D **7**, 201 (1983).

[46] F. Takens, in *Dynamical Systems and Turbulence*, edited by D.A. Rand and L.-S. Young, Lecture Notes in Mathematics, Vol. 898 (Springer, Berlin, 1981), pp. 366–381.

[47] R. Wackerbauer, A. Witt, H. Atmanspacher, J. Kurths, and H. Scheingraber, Chaos, Solitons Fractals **4**, 133 (1994).

[48] B. McMillan, Ann. Math. Stat. **24**, 196 (1953).

[49] C.E. Shannon and W. Weaver, *The Mathematical Theory of Communication* (University of Illinois Press, Urbana, 1949), reprint 1963.

[50] A. Rényi, *Probability Theory* (North-Holland, Amsterdam, 1970).

[51] P.I. Saparin, A. Witt, J. Kurths, and V. Anishchenko, Chaos Solitons Fractals **4**, 1907 (1994).

[52] E.M. Bollt, T. Stanford, Y.-C. Lai, and K. Życzkowski, Phys. Rev. Lett. **85**, 3524 (2000).

[53] W.H. Press, S.A. Teukolsky, W.T. Vetterling, and B.P. Flannery, *Numerical Recipies in C*, 2nd ed. (Cambridge University Press, New York, 1996), reprinted 1996.

[54] C. Beck and F. Schlögl, *Thermodynamics of Chaotic Systems.*

An Introduction, Cambridge Nonlinear Science Series Vol. 4 (Cambridge University Press, Cambridge, England, 1993), reprinted 1997.

[55] X. Pei and F. Moss, Nature (London) **379**, 618 (1996).

[56] *Mathematik Handbuch für Technik und Naturwissenschaft*, edited by J. Dreszner (Harry Deutsch Verlag, Thun, 1975).

[57] For a general discussion of aperiodic signals fed into threshold devices, see Refs. [23–25,55].